

# Preamplifier for ALICE-PHOS project (CERN)

## Calculation and design.

*R. Rongved, A. Klovning, O. Maeland*

*University of Bergen, Norway.*

*and*

*I. Sibiriak*

*Russian Scientific Centre " Kurchatov Institute ", Moscow, Russia.*

### Introduction.

A design of a Charge Sensitive Preamplifier ( *CSP* ) to be used for the ALICE photon spectrometer (PHOS) is given.

PHOS will consist of 36000 detectors each containing a PBWO crystal, a *PIN* photodiode and preamplifier as the readout channel.

We will give the results of a detailed calculation of equivalent noise charge (*ENC*) in frequency and time domain taking into account the stages following the *JFET*'s, gain and the output rise time. The comparison with the experimental results will also be given.

### 1. Preamplifier.

For transforming the *PIN* photodiode signals into the form suitable for the digitisation one has to use a *CSP* and shaper. Bearing in mind the energy resolution as well as the PHOS sector design, we came to the following requirements for preamplifier parameters ( *PIN* photodiode with active window 17mm x 17mm connected to *CSP* ) :  $ENC < 600e$  , power consumption  $< 200mW$  , dimension - 20mm x 20mm x 20mm or less.

The developed *CSP* design is shown in Fig1.1.

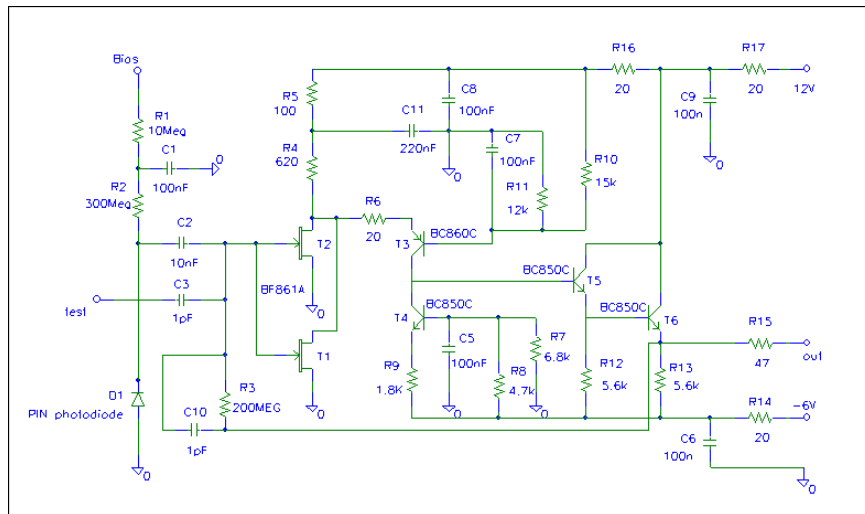


**Fig.1.1 Preamplifier**

The preamplifier is an operational amplifier with the feedback capacitor *C10* and field-effect transistors *T1* and *T2* at the input. The resistor *R3* is direct current feedback and determines the fall time of the *CSP*'s output signal ( 200• S for our case ). The drain of *T1* and *T2* feeds the emitter of transistor *T3*, whose base potential determines the operation voltage of the *JFET*'s. The operating currents of *T1* and *T2* are determined by the resistors *R4* and *R5*. The characteristics of the *JFET*'s determines the preamplifiers noise level and the output pulse rise time.

It is important that the charge sensitivity depends on the capacitor  $C10$  only. To achieve this it is necessary that the  $CSP$  gain without feedback is approximately equal to 3000. To satisfy these requirements the scheme where the current generator  $T4$  is the load for  $T3$  was chosen. For circuit stabilisation the  $CSP$  consist of two stages. The emitter followers  $T3$  and  $T6$  decrease the influence of output termination. The power consumption is dependent on the choice of working points for the transistors. The  $CSP$  is supplied from +12volt and -6volt.

## 2. Noise sources

Fig. 2.1 shows the equivalent input circuit for studying the energy resolution capabilities of the preamplifier.

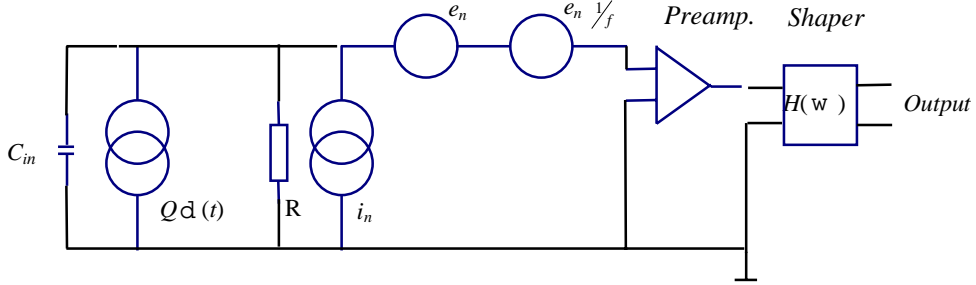


Fig 2.1

The various noise elements are the following [1-5]:

- The noise developed in the first amplifying devices (FET) produces a *RMS* voltage noise  $\langle \hat{e}_n \rangle$ . This source of noise can be represented by Johnson noise in the equivalent series resistor  $R_s$  and has the value

$$\langle \hat{e}_n \rangle = 4kT R_s Df, \quad (2.1)$$

where  $k$  = Boltzman's constant,  $T$  = equivalent temperature of  $R_s$ , and  $Df$  = unit band width.

- The detector leakage current  $i_D$  and the input current,  $i_g$ , to the first amplifying device can be represented by a *RMS* current noise as

$$\langle \hat{i}_n \rangle = 2q \langle \hat{i}_D + i_g \rangle Df, \quad (2.2)$$

where  $q$  = electronic charge.

- The parallel resistance noise  $\langle \hat{e}_n \rangle_R$  arise from any resistor,  $R$ , shunting the input circuit and we can regard the voltage source as a current source which must be included in the value of the current generator  $\langle \hat{i}_n \rangle_R^2$  in (2.2). The increase in  $\langle \hat{e}_n \rangle_R^2$  due to this is

$$\langle \hat{e}_n \rangle_R^2 = \frac{4kT}{R} Df. \quad (2.3)$$

- The so-called flicker noise is usually represented by a noise voltage generator in the the input lead having the value

$$\hat{e}_n \hat{f}_{1/f} = \frac{A}{2\pi f} \text{Df} , \quad (2.4)$$

where  $A$  is the power spectral density constant for  $1/f$  noise.

- The parallel lossy dielectric noise as described by Radeka [12] and Llacer [13] can be expressed as follows

$$\hat{e}_n \hat{f}_L = \frac{A_L}{2\pi f C_{in}} \text{Df} , \quad (2.5)$$

where  $C_{in}$  is the total input capacitance and  $A_L$  is the power spectral density constant for parallel lossy dielectric noise.

For the detector signal approximating an impulse of current containing charge  $Q$ , the signal at the input then approximates a voltage step function of magnitude  $Q/C_{in}$ .

The equivalent noise charge (*ENC*) of preamplifier plus shaper is defined as the charge (in coulombs or number of electrons) that, when put into  $C_{in}$ , gives an output pulse height equal to the *RMS* value of the output noise generator.

$$\hat{e}_n \hat{f}_p = 4kT \frac{qI}{2\pi kT} + \frac{1}{R} \frac{1}{2\pi f C_{in}} \text{Df} , \quad (2.6)$$

where  $I = i_D + i_g$ . Then summed up the noise voltage at the input of the preamplifier will be

$$E^2 \hat{w} = \hat{e}_n \hat{f}_S + \hat{e}_n \hat{f}_p + \hat{e}_n \hat{f}_{1/f} . \quad (2.7)$$

For transformation  $E^2 \hat{w}$  to the noise charge, one needs to multiply eq.(2.7) by  $C_{in}^2$

$$Q^2 \hat{w} = C_{in}^2 E^2 \hat{w} = N_S C_{in}^2 + \frac{N_p}{2\pi^2} + \frac{N_{1/f}}{f} \text{Df} , \quad (2.8)$$

where

$$\begin{aligned} N_S &= 4kT R_S \\ N_p &= 4kT \frac{qI}{2\pi kT} + \frac{1}{R} \\ N_{1/f} &= A C_{in}^2 + A_L \end{aligned}$$

### 3. Calculation of *ENC*

#### 3.1 Calculation of the *ENC* in a frequency domain

The classical method of calculating the *ENC* is based on integrating the output response function in a frequency domain. If it is assumed that the response of the shaper to a sine wave of frequency  $w/2p$  is  $H \hat{w}$ , and that a input voltage pulse has a maximum amplitude  $A_{max}$  at the output of the filter, then

$$ENC = \frac{1}{2\pi A_{max}^2} \int_0^{\infty} Q^2 |H(w)|^2 dw \propto \frac{1}{\beta^{1/2}}. \quad (3.1)$$

The shaper is of great importance in determining the energy resolution capabilities of the spectrometer and the associated electronics. With regard to the signal to noise ratio, a theoretical study by den Hartog and Muller [6] shows that, considering the relative spectral distribution of serial and parallel noise, the best signal to noise ratio is obtained with a shaper having a cusp shaped response to a input voltage pulse.

When the time constant of the shaper is optimised, the optimum value of the  $ENC$  is shown to be

$$ENC_{cusp} = \sqrt{4kTC_{in}} \frac{R_s}{R}^{1/4}. \quad (3.2)$$

With the condition that the input of the shaper match the time constant

$$\tau_1 = \tau_0 = C_{in} \sqrt{R_s R}, \quad (3.3)$$

where  $\tau_0$  is the so-called noise corner time constant.

Among various shapers single  $CR$  differentiation of time constant  $\tau_1$  and  $n$  stage  $CR$  integration of time constant  $\tau_2$  are widely used because of their good noise performances and ease of construction. The equivalent schematic of these shapers is shown in Fig. 3.1.

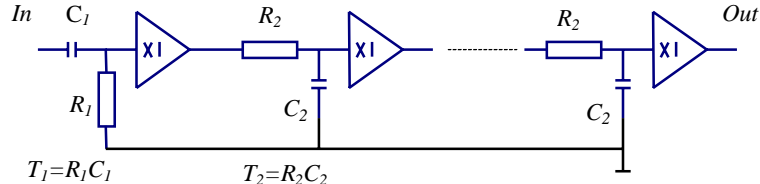


**Fig. 3.1**

Nowack [7] showed by numerical calculation that for  $n = 1-5$ , the  $ENC$  always gives the minimum value for  $\tau_1 = \tau_2 = \tau_{opt}$  and

$$\tau_{opt} = \frac{\tau_0}{\sqrt{2n-1}}. \quad (3.4)$$

In the following discussions we will limit ourselves to the case where  $\tau_1 = \tau_2 = \tau$  and  $n = 1, 2, 4$ .

Using Fig. 3.1 and Laplace transform with respect to an input step pulse one finds

$$H(p) = \frac{1}{p} \frac{p}{(p+1/\tau)} \frac{1}{\tau(p+1/\tau)}. \quad (3.5)$$

From eq. (3.5) using  $p = j\omega$  we obtain

$$|H(\omega)|^2 = \frac{\omega^2 \tau^2}{(1 + \omega^2 \tau^2)^2} \quad (3.6)$$

and using the inverse Laplace transformation with respect to time one finds

$$H(t) = \frac{t}{\ln t} e^{-\frac{t}{\ln t}}. \quad (3.7)$$

To calculate the *ENC* from eq. (3.1) one needs to know  $A_{max}$ . This can be done by finding maximum of  $H(t)$  using eq. (3.7). This gives  $T_M = nT$  and

$$A_{max} = \frac{n}{\ln n!} e^{-n}. \quad (3.8)$$

For  $n = 1, 2, 4$   $A_{max}$  is 0.37, 0.27, 0.20 accordingly.

As an example we will calculate the *ENC* for a shaper with  $n = 4$ . Using eqs.(3.6) and (2.8) and  $A_{max} = 0.20$  into eq.(3.1) and we find

$$ENC = \frac{0.257}{\tau} N_S C_{in}^2 + 1.8\tau N_P + 3.29 N_{1/f} \frac{\phi}{\tau}^{1/2}. \quad (3.9)$$

In eq. (3.9) the numbers  $N_S, N_P, N_{1/f}$  are weight constants for the noise characteristic of the shaper. The values of these are

$$N_S = 0.257/\tau, N_P = 1.8\tau, N_{1/f} = 3.29. \quad (3.10)$$

Fig 3.2 shows the *ENC* for serial-, parallel- and  $1/f$ -noise vs.  $\tau$ .

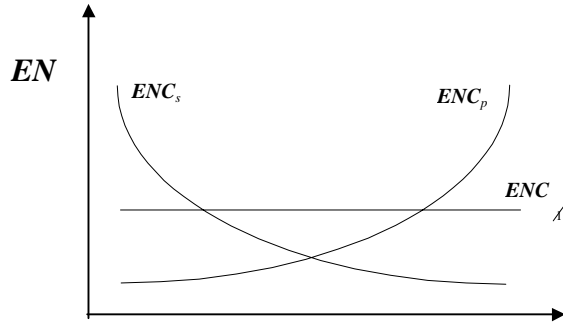


**Fig. 3.2**

Often one will express the relative noise performance of any shaper as “cusp factor”  $F$  which is defined as

$$F = \frac{ENC}{ENC_{cusp}}. \quad (3.11)$$

Without  $1/f$ -noise the formula for  $F$  is

$$F = \sqrt{2} \sqrt[4]{N_S N_P}.$$

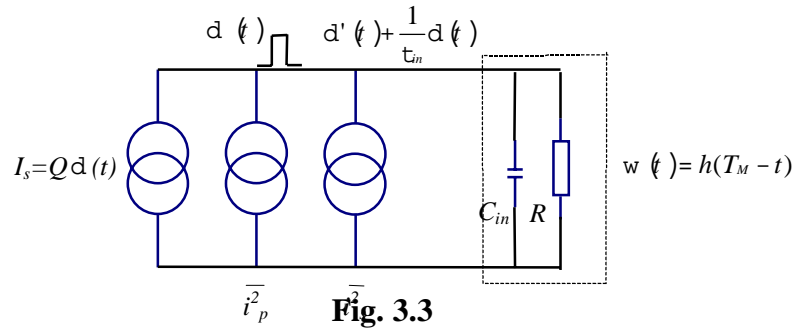
The values for  $N_S, N_P, N_{1/f}, F$ , peaking time  $T_M$  and optimal time constant  $\tau_{opt}$  is shown in Table 1.

Table 1.			
$n$	1	2	4
$N_S$	$0,92/\tau$	$0,43/\tau$	$0,26/\tau$
$N_P$	$0,92\tau$	$1,28\tau$	$1,8\tau$
$N_{1/f}$	3,69	3,43	3,29
$F$	1,36	1,22	1,17
$T_M$	$\tau_0$	$1,15\tau_0$	$1,51\tau_0$
$\tau_{opt}$	$\tau_0$	$0,56\tau_0$	$0,38\tau_0$

### 3.2 Calculation of $ENC$ in the time domain

Calculation of  $ENC$  in the time domain is more clear because the timing parameters of the shaper can easily be observed by an oscilloscope. Moreover the time variant shaper such as ORTEC 673 can be calculated only in the time domain.

The noise sources and the shaper in the time domain is shown in Fig. 3.3.



According to [8,9] we can think of parallel noise as a random sequence of current pulses (delta functions). In the same way we can think of the serial noise as random sequences of voltage pulses. The serial noise can also be represented by a current generator in parallel with the R-C network, as shown in Fig. 3.3. The current noise spectrum is obtained by multiplication by  $C_{in} j w + \frac{1}{t_n} \delta(t)$ , where  $t_n = C_{in} R$ . Consequently each voltage impulse  $V_0 d(t)$  is converted to

$$V_0 C_{in} \frac{\delta}{\delta} d(t) + \frac{d(t) \delta}{t_n} \frac{\delta}{\delta},$$

the sum of a doublet and a pulse.

The  $ENC$  is obtained by adding up independent contributions to the shaper output from all pulses and doublets, according to the Cambell's theorem.

The serial-noise is found as

$$ENC_S^2 = \frac{1}{2} \int_{t_n}^{\infty} C_{in}^2 \frac{d^2}{dt^2} V(t) + \frac{1}{t_n} \int_{t_n}^{\infty} \frac{d^2}{dt^2} V(t) dt \quad (3.12)$$

and the parallel-noise

$$ENC_P^2 = \frac{1}{2} (\bar{i}_n)^2 \int_{-\infty}^{+\infty} [W(t)]^2 dt, \quad (3.13)$$

were:

$$\begin{aligned} e_n &= RMS \text{ serial-voltage-noise per } \sqrt{Hz}, \\ i_n &= RMS \text{ parallel-current-noise per } \sqrt{Hz}. \end{aligned}$$

The weight function  $W(t)$  represents the residual effect at  $T_M$  (measuring time) of a single unit amplitude step (parallel) noise at time  $t$  before  $T_M$ .  $W'(t)$  is the differential of  $W(t)$  and represents the residual effect at  $T_M$  of a single unit amplitude delta (serial) noise. For the time invariant shaper  $W(t) = H(t)$ . The expressions under the integrals in eqs. (3.12) and (3.13) are the weight functions  $M_S$  and  $M_P$  accordingly. As in the frequency domain, the time domain the weight function is normalised to its maximum value so that the impulse signal (charge) from the detector is recorded with a weight of unity. The limit of integration  $-\infty$  to  $+\infty$  imply that the integration is carried out for all non-zero of  $W(t)$  and  $W'(t)$ .

We will now calculate  $M_S$  and  $M_P$  in the time domain for a shaper with  $n = 4$ . From eqs.(3.7) and (3.8) we have

$$W(t) = \frac{H(t)}{A_{max}} = \frac{t}{\pi n t} e^{\frac{n-t}{\pi t}} \quad (3.14)$$

and for  $n = 4$

$$\begin{aligned} W(t) &= \frac{t}{\pi 4 t} e^{\frac{4-t}{\pi t}}, \\ W'(t) &= \frac{e}{\pi 4 t} \left[ \frac{4}{\pi 4 t} e^{\frac{-t}{\pi t}} - t^3 e^{\frac{-t}{\pi t}} \right] \frac{1}{\pi t}. \end{aligned}$$

From eqs.(3.12) and (3.13) we find

$$M_P = \frac{1}{2} \int_{-\infty}^{+\infty} \frac{t}{\pi 4 t} e^{\frac{4-t}{\pi t}} dt = \frac{1}{2} \frac{e}{\pi 4 t} \left[ \frac{8!}{\pi t} \right] = 1.8 t$$

and

$$M_S = \frac{1}{2} \int_{-\infty}^{+\infty} [W'(t)]^2 dt = \frac{1}{2} \left[ \frac{4! 6!}{\pi t} - \frac{8! 7!}{\pi t^2} + \frac{8! 8!}{\pi t^3} \right] = \frac{0.257}{\pi t}.$$

We have obtained the same result as calculating in the frequency domain (see table 1).

### 3.3 The practical calculation of *ENC*

The practical calculation of *ENC* of the designed preamplifier have been carried out by using

$$ENC = \frac{1}{q} \frac{\phi}{2kT} N_S C_{in}^2 M_S + N_P M_P + BN_f M_{\frac{1}{f}} \frac{\phi}{2kT}^2 \quad (3.15)$$

obtained from eqs.(2.8) and (3.9). In eq. (3.15) we have

$$\begin{aligned} N_S &= 4kTR_S \\ N_P &= \frac{\phi qI}{2kT} + \frac{1}{R} \frac{\phi}{2kT} 4kT \\ N_f &= 2 \cdot 10^{-4} C_{in}^2 + 2 \cdot 10^{-34} \end{aligned} \quad (3.16)$$

where constants for  $N_f$  was taken from [13] and  $B$  is the number of FET's connected in parallel. To calculate  $R_S$  taking into account the stages following the FET's and using the diagram in Fig. 3.4 based on the layout in Fig. 1.1 where  $R_{Si}$  and  $R_{Pi}$  are serial and parallel noise resistance of the  $T1,3,4,5$ .

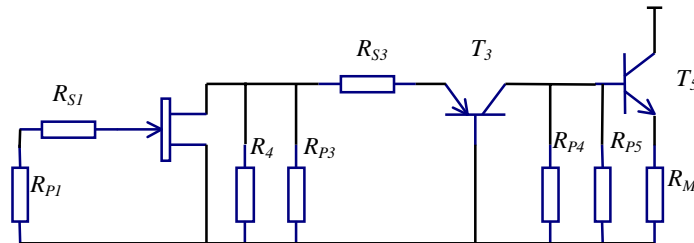


Fig. 3.4

The noise resistances are

$$\begin{aligned} R_{S1} &= \frac{0.7}{g_m} = 50\text{W} \quad \text{for } g_m = 14\text{mA/V} \quad (1 \text{ FET}) \\ &= 24\bullet \quad \text{for } g_m = 29\text{mA/V} \quad (2 \text{ FETs}) \end{aligned}$$

$$R_{S3} = \frac{r_e}{2} + r_b @ 100\text{W}$$

$$R_{P3} = R_{P5} = 2\text{br}_e @ 5\text{kW}$$

$$\frac{1}{R_{P4}} = \frac{1}{10} \frac{2qI_4}{4kT} = 1.9 \cdot 10^{-3} \text{ W}$$

where:

$r_e$  and  $r_b$  are the emitter and base domain resistances of the transistor;

$g_m$  is the FET transconductance

$I_4$  is the collector current in  $T_4$

$b$  is the transistor current gain.

The value of  $R_s$  can be calculated [11]

$$R_s = R_{S1} + \frac{1}{g_m^2} \frac{1}{R_4} + \frac{1}{R_{P3}} + \frac{1}{R_{P5}} + R_{S3} \frac{1}{g_m R_i} + \frac{1}{g_m R_4} + \frac{C_{gd}^2}{C_{in}} , \quad (3.17)$$

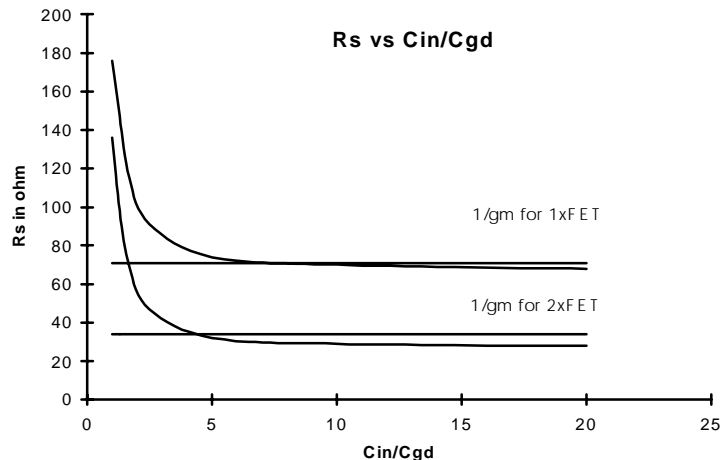
where:

$R_i$  is the FET output resistance @ 10kW ,  
 $C_{gd}$  is the FET gate to drain capacitance.

A good approximation for calculating  $R_s$  is

$$R_s = \frac{1}{g_m} . \quad (3.18)$$

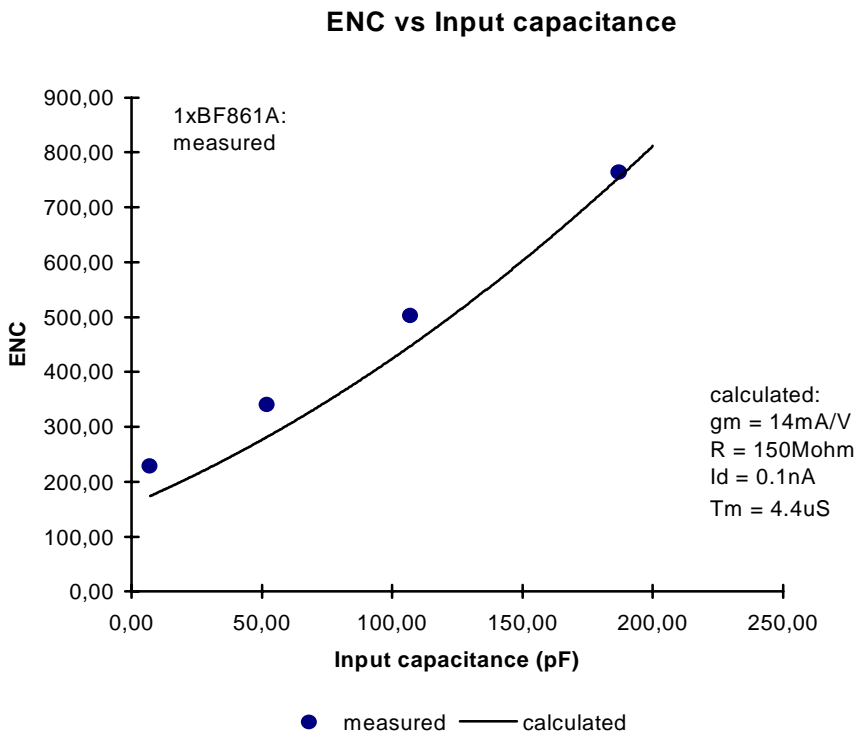
Fig.3.5 shows the calculated curves of  $R_s$  for 1 and 2 FETs vs.  $C_{in}/C_{gd}$  using eqs. (3.17) and (3.18).



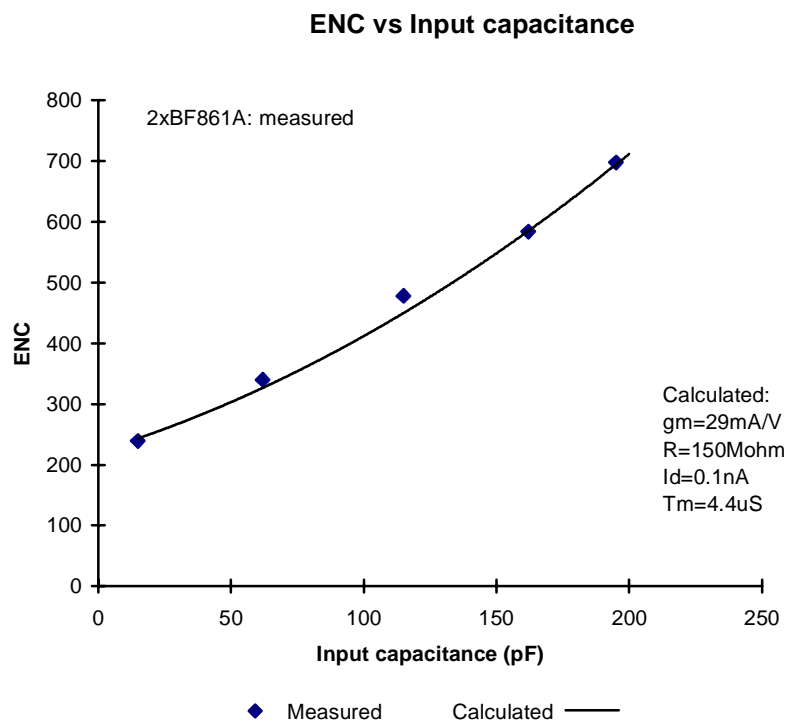
**Fig.3.5**

Fig.3.5 shows that eq. (3.18) may be used for  $C_{in}/C_{gd} > 5$ . In the calculation of ENC we used  $R = 150$  M $\Omega$  , the shaper with  $n = 4$ ,  $T_M = 4.4 \mu$  S and  $I = 0.1$  nA.

Figs.3.6 and 3.7 shows the calculated (from eqs.(3.15), (3.16) and (3.17)) and measured curves of ENC vs. the input capacitance for 1 and 2 FETs.

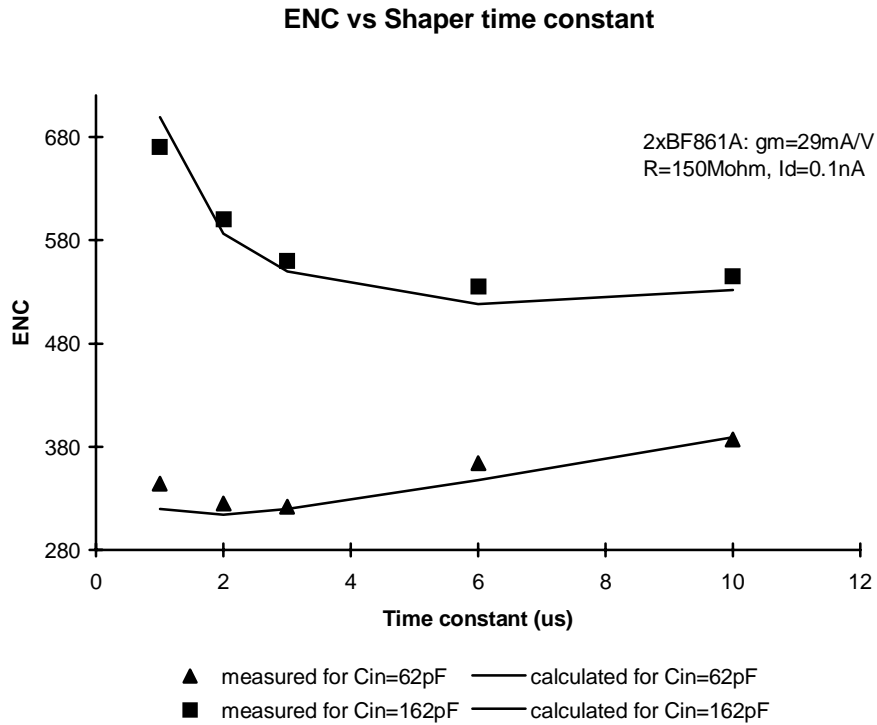


**Fig.3.6**



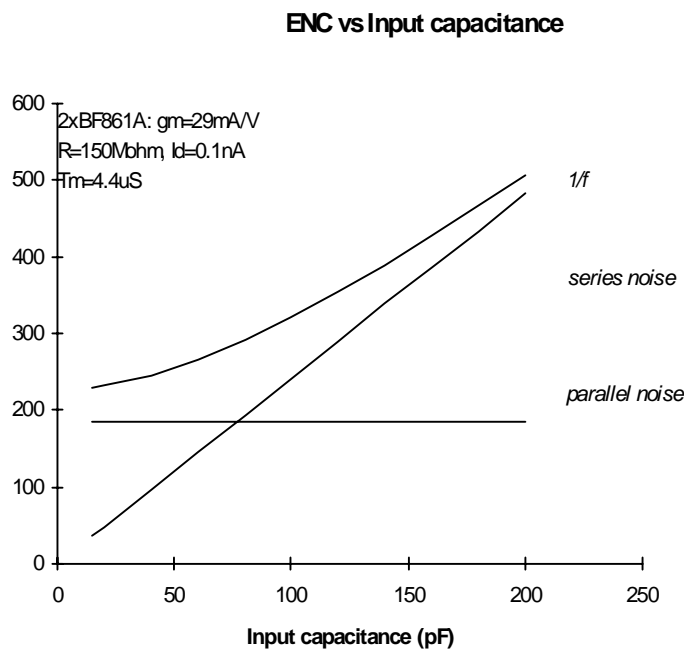
**Fig.3.7**

Fig. 3.8 show the calculated and measured curves for  $ENC$  vs. shaping time constants for 2 FETs in parallel.



**Fig.3.8**

Fig.3.9 shows the calculated curves of the *ENC* for each noise source vs. the input capacitance for 2 FETs. It is seen that the dominant noise is in our case is  $1/f$ .



**Fig. 3.9**  
**4. Influence gain on preamplifier parameters**

The value of the gain,  $K$ , without feedback is dependant on the charge sensitive temperature instability, the rise time and the value of the dynamic capacitance.

The charge sensitive can be calculated as

$$Z = \frac{K}{C_{in} + C_{fb} (K + 1)}, \quad (4.1)$$

where  $C_{fb}$  is the feedback capacitor. If  $K \gg C_{in}/C_{fb}$  then  $Z = 1/C_{fb}$  and the charge sensitive is determined by only a passive element.

The charge sensitive temperature insabilities is according to eq.(4.1)

$$\frac{1}{Z} \frac{dZ}{dT} = \frac{1}{1 + Kb} \frac{1}{K} \frac{dK}{dT} - \frac{1}{C_{fb}} \frac{dC_{fb}}{dT}, \quad (4.2)$$

where  $b = C_{fb}/C_{in}$ . The temperature coefficient of the the capacitor is

$$\frac{1}{C_{fb}} \frac{dC_{fb}}{dT} \gg 0.5 \cdot 10^{-5}.$$

The temperature coefficient of the gain with the FET at the input is

$$\frac{1}{K} \frac{dK}{dT} \gg 0.5 \cdot 10^{-2}.$$

To have the best noise performance one has to fulfill the following conditions;  $1 + Kb \neq 100$  and  $K \neq 100/b = 100C_{in}/C_{fb}$ . When  $C_{fb} = 1\text{pF}$  and the PIN capacitance  $C_{in}$  is equal to  $160\text{pF}$  then  $K > 1600$ .

The rise time constant can be calculated to be

$$\tau_F = \frac{\tau}{1 + Kb} @ \frac{R_K C_t}{g_m R_K (C_{fb}/C_{in})} = \frac{C_{in} C_t}{g_m C_{fb}}, \quad (4.3)$$

where  $R_K$  and  $C_t$  are the equivalent resistanse and stray capacitance at the connecting piont of the collectors of T3 and T4. The rise time is  $t_F = 2.2\tau_F$ .

If one needs a small rise time  $t_F$  to be used with a large detector, an additional stage  $Q5$  must be added as shown in Fig.5.2. Then the gain can be calculated as

$$K = g_m R_K \frac{R_4}{r_{ea} + R_6 + r_{e3}}, \quad (4.4)$$

where  $r_{ea}$  and  $r_{e3}$  are the emitter domain resistance in  $Q5$  and  $Q3$  respectively. Then the expession for  $\tau_F$  is

$$\tau_F = \frac{R_6 + r_{ea} + r_{e3}}{g_m R_4} \frac{C_t C_{in}}{C_{fb}}. \quad (4.5)$$

Fig.4.1 shows the calculated and measured curves of  $t_F$  vs.  $C_{in}$  for the amplifier with and wihtout the additional stage. The measured values of  $t_F$  is  $18\text{ns}$ .

Rise time vs Input capacitance (pF)

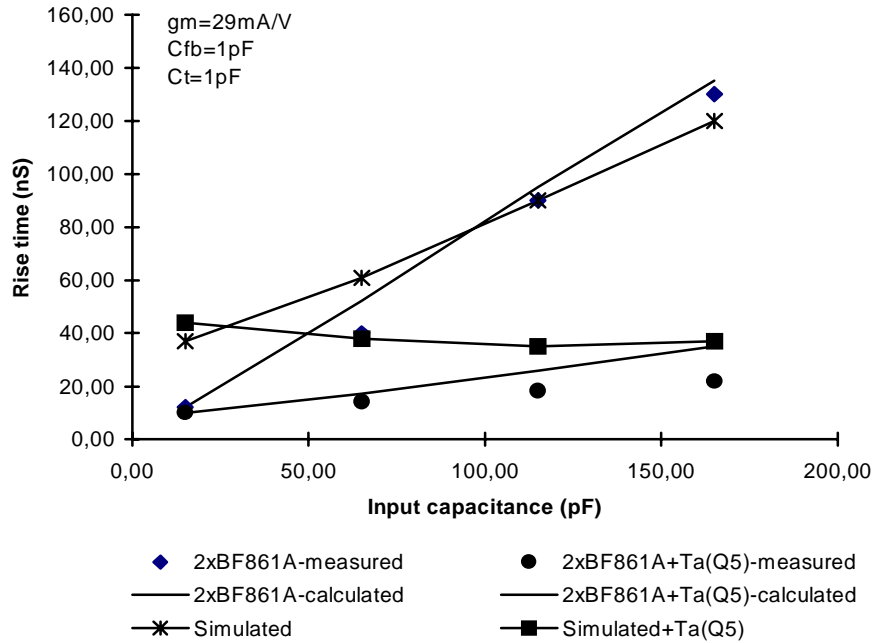


Fig.4.1

## 5. Simulation

Simulations of the preamplifier were performed on the diagrams presented in Figs.5.1 and 5.2. Fig.5.2 includes the extra stage  $Q5$ . The simulations were done with SPICE. Results from simulations are included in Figs. 4.1 and 5.3

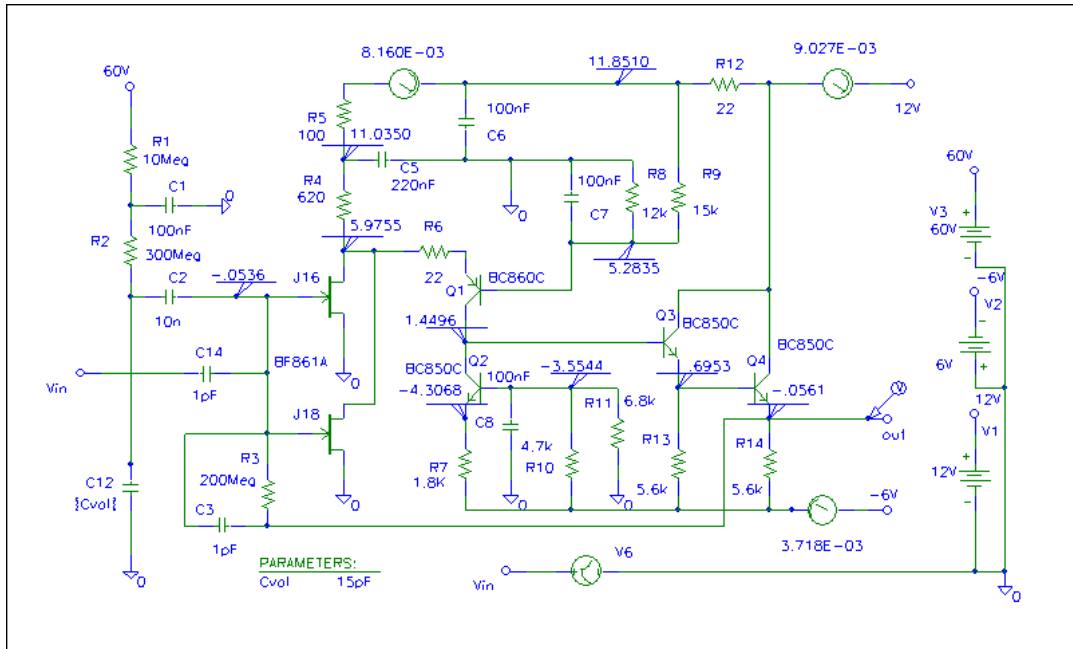


Fig. 5.1

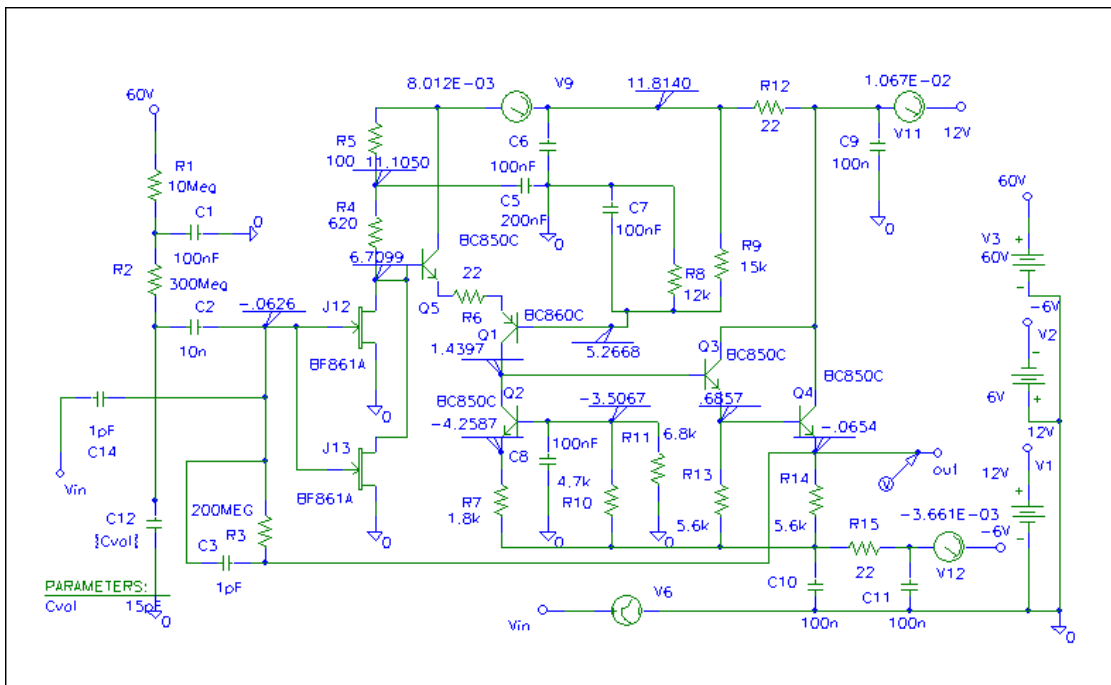


Fig. 5.2

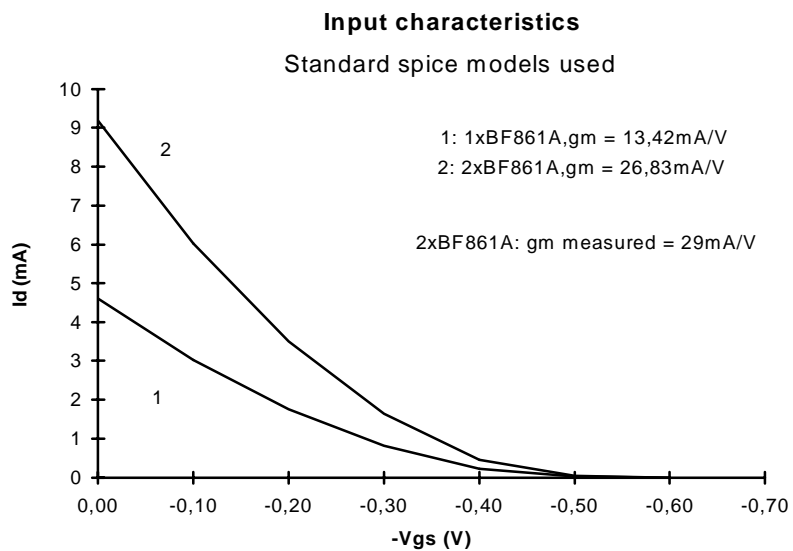
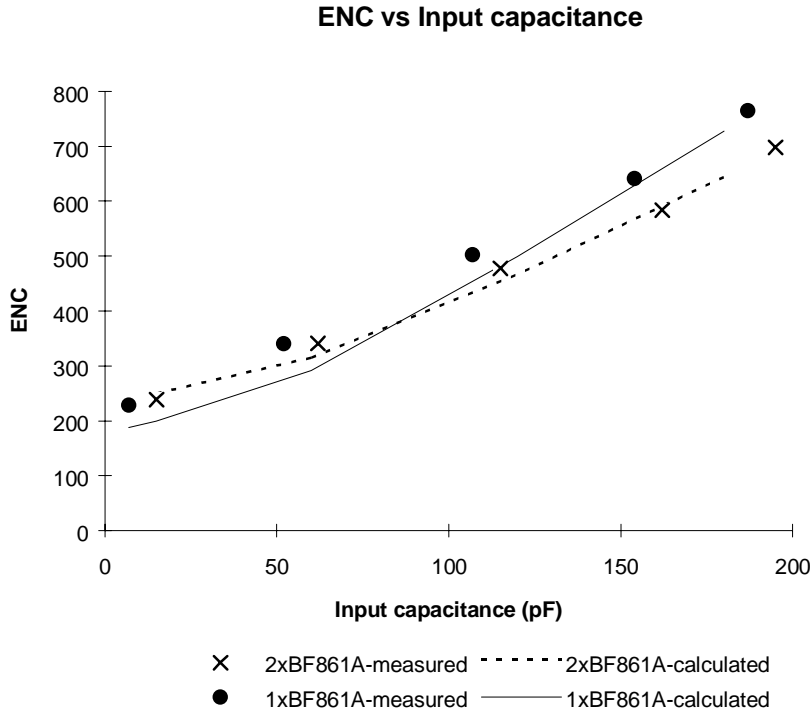


Fig. 5.3

## 6. Conclusion

The designed preamplifier can be used with a wide range of PIN-diodes and semiconductor detectors. The preamplifier with one FET on the input has the best noise level for detectors with capacitances  $< 100\text{pF}$ . The preamplifier with 2 FETs on the input connected in parallel is the best one for detectors with capacitance  $> 100\text{pF}$ . This is shown in Fig. 3.6 and 3.7.



**Fig. 6.1**

Using the parallel connected FETs for increasing the transconductance  $g_m$  with the aim of getting the best noise resolution is better than using one FET with the same  $g_m$  but which demand more drain current,  $I_d$ . This is shown in Fig. 6.1 as  $ENC$  vs. input capacitance  $C_{in}$  for BF861B with  $g_m = 21\text{mA/V}$  and  $I_d = 12\text{mA}$ , for two BF861A connected in parallel we have in total  $g_m = 29\text{mA/V}$  with  $I_d = 7.5\text{mA}$ . The preamplifier with two parallel connected FETs has a power consumption of  $150\text{mW}$ , while the one with one FET tested in 1995-96 used  $250\text{mW}$ . This is an important parameter for PHOS since the calorimeter is designed to work at  $\approx -20\text{ C}$ . Adding the stage  $Q5$  as indicated in Fig.5.1 allow a marked decrease in the rise time of the output pulse from the preamplifier, this can be used for timing measurements.

In Fig.3.8 is shown that the  $1/f$  noise is the dominant one. This noise is mainly determined by the technology of making FET. So for further decrease of the preamplifier noise this will be connected with improvement of the technology of making the FET.

The designed preamplifier satisfy the demands for PHOS and is produced for test modules of the PHOS calorimeter.

## References

- [1] P.W. Nicholson, Nuclear Electronics (Wilay, New York, 1973).
- [2] E. Baldingez and W. Franzen, Advances in Electronics and Electron Physics (Academic Press, New York, London, 1956) p.255.
- [3] A.B. Gillespie, Signal, Noise and Resolution in Nuclear Counter Amplifiers (Pergamon Press, London, New York, 1953).
- [4] F.S. Goulding and W.I. Hansen, Nucl. Instr. and Meth. 12(1961) p.249.
- [5] H. Murakami, Nucl. Instr. and Meth. A243(1985) p.132.
- [6] H. Den Hartog and F.A. Muller, Physica 13, No.9 (Nov.1947).
- [7] G. Nowack and J.W. Klein, Proc. 2nd ISPRA Nuclear Electronics Symposium (1975) p.87.
- [8] M. Konrad, IEEE Trans. Nucl. Sci. 1968 v.NS-15, No.1, p.268.
- [9] V. Radeka, IEEE Trans. Nucl. Sci. 1974 v.NS-21, No.1, p.51.
- [10] E.P. Dementiev, Elements of the common theory and calculation of noisy linear chains, (Moscow, 1963).

- [11] Y.K. Akimov et. al., Semiconductor detectors in Experimental Physics, (Moscow, 1989), p226.
- [12] V. Radeka, IEEE Trans. Nucl. Sci. 1969 v.NS-16, No.5, p.17.
- [13] J.Llacer, Nucl. Instr. and Meth. 130(1975) p.565.